Introduction to Remote sensing and applications

Dr.Weerakaset Suanpaga

D.Eng(RS&GIS)

Contents

Application of Remote Sensing

Advantage of RS

- Wide Coverage, Periodical Observation
- Variety of Observing Method
- Multi-resolution – Multi-temporal – Multi-spectral
- Global Environment – Local Application
- Hydrology, Oceanography, Global Env. Study, CO2

Advantage of RS con't

- Agriculture, Forestry, Fisheries, Ecological Mapping
- Coastal zone management, Health Management, Energy
- Fire, Oil-spill, Volcano, Earthquake, Flood, Ice,
- Land use mapping, Cadastral Mapping, Topographic Map, Change Detection
- Military
- Use wisely by understanding advantage and limitation

Recent an example of RS application

0 Base map/Back Ground map integrate with web-map server

1. Remote Sensing (LIDAR) for Management of Highway Assets for Safety
2. 3D Model of University of Melbourne Campus
3. NOAA/AVHRR - MODIS/TERRA Reception, Archiving and Distribution
4. Forest Fire Monitoring from NOAA AVHRR
5. MODIS for Flood Monitoring
6. Landuse Classes and its Multi-temporal Spectral Curves
7. planting pattern detection
8. Forest Fire Monitoring from NOAA AVHRR-Thailand
9. **Defense Meteorological Satellite Program[DMSP]**
10. **Rice Growth Monitoring using RADAR Remote Sensing**

Recent an example of RS application

11. RS for Drought Monitoring (using NOAA AVHRR) in Indonesia
12. Soil-Water-Atmosphere-Plant Model (SWAP)
13. Soil Erosion Monitoring
14. Tea yield Model
15. Mt. Mayon Volcano Comprehensive Disaster Prevention Master Plan
16. Flood Monitoring using JERS
17. Bangkok Urban Area Expansion
18. Micro Air Vehicles (MAV)
19. GPS
20. Debris flow
21 Urban heat Island

Base map Web map server

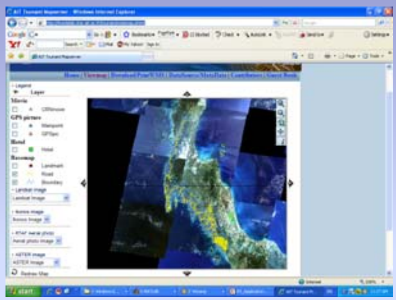

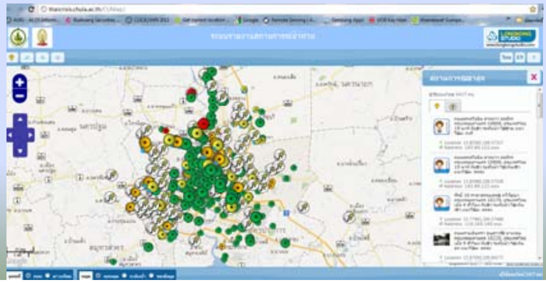

Remote Sensing (LIDAR) for Management of Highway Assets for Safety

Iowa Department of Transportation

<u>Iowa State University</u> ~ University of Missouri-Columbia Lincoln University ,University of Missouri-Kansas City University of Missouri-St. Louis,University of Northern Iowa

Main objective

Utilize light detection and ranging (LIDAR) technology to obtain highway safety-related information.

The safety needs of older drivers in terms of prolonged reaction times were taken into consideration.

(1) identification of crashes that older drivers are more likely to be involved in,
(2) identification of highway geometric features that are important in such crashes
(3) utilization of LIDAR data for obtaining information on the identified highway geometric features
(4) assessment of the feasibility of using LIDAR data for such applications.

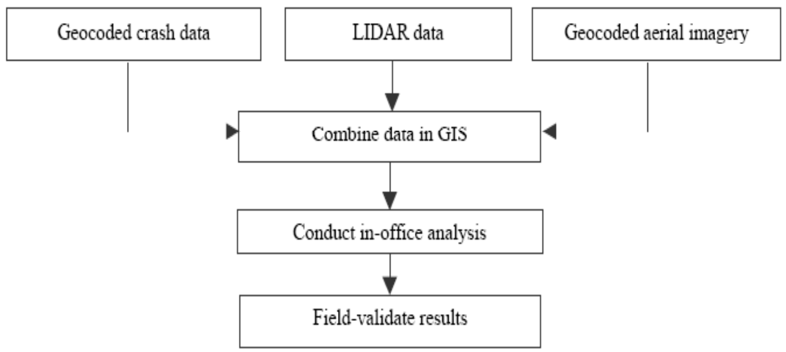

Figure 3.1. Adopted research methodology

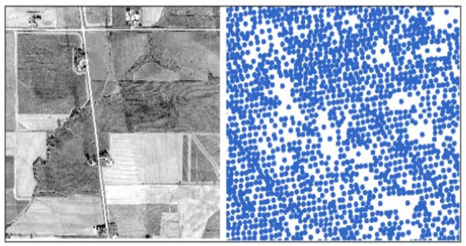

Figure 3.3. Sample orthophoto and converted LIDAR data

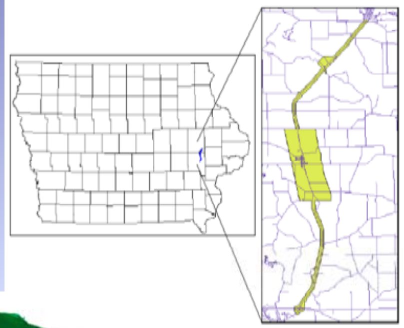

Figure 3.2. Study corridor

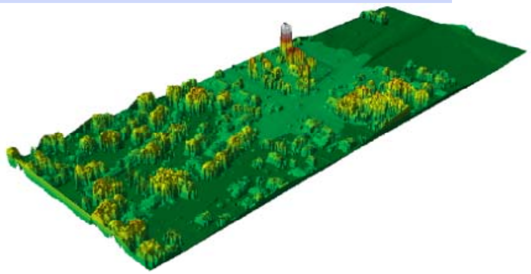

Figure 3.4. Sample 3D TIN of the study corridor passing through Solon, Iowa

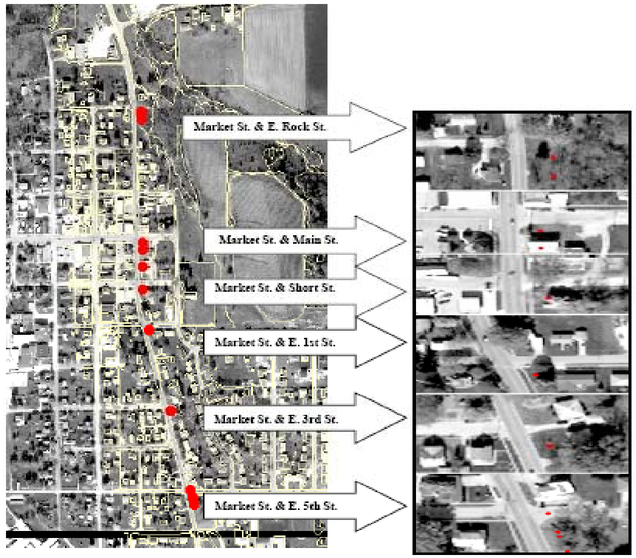

Figure 4.1. Six selected intersections and crash locations

Figure C.4. Stopped driver's view at the intersection of Market St. and Main St.

Figure C.1. Stopped driver's view at the intersection of Market and East Fifth streets

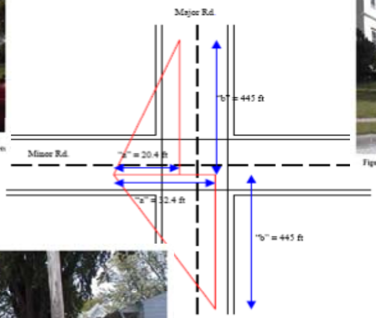

Figure C.3. Stopped driver's view at the intersection of Market St. and Short St.

Figure C.2. Stopped driver's view at the intersection of Market St. and E. First St.

Sight triangles for Case B1, left turn from the minor road

The distance of the detected potential obstructions refers to the distance of the blue dots obtained during the line-of-sight analysis from the driver stopped on the minor road

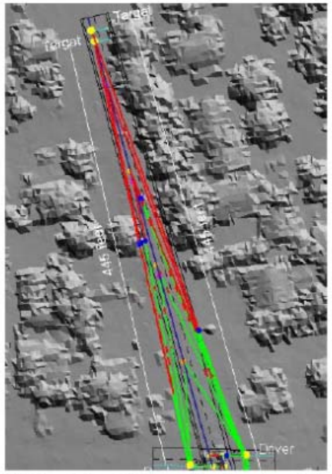

Figure 4.2. Multiple lines of sight at 100-ft interval along the major road (Market St. and E. Fifth St.)

Sixty-nine LIDAR bounds superimposed on 12 orthophoto bounds

summary

-66 potential sight distance obstructions→ identified by the line-of-sight

-The intersection with the highest crash frequency involving older drivers was correctly found to have obstructions located within the intersection sight triangles.

-LIDAR data can be utilized for identifying potential sight distance obstructions at intersections. The safety of older drivers can be enhanced by locating and rectifying intersections with obstructions in sight triangles. $30,000 was spent

Melbourne *Ikonos* Test Field

- 3-fold image coverage
- 7km x 7km area (Δh < 100m)
- 40 GPS surveyed GCPs
- 19 building control pts.
- sub-pixel, multi-measurements to image features
- 2D & 3D point
- s
- for 2D
- n tests

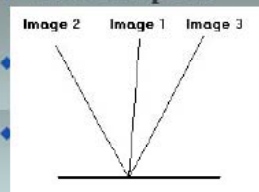

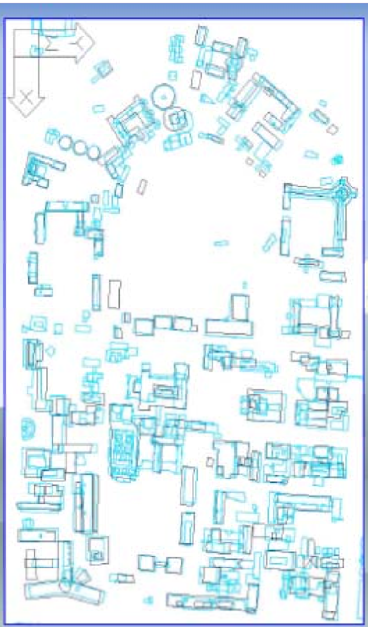

Building Extraction Completeness

Ikonos 1m Pan Stereo versus Aerial Photography (1:15K)

- Loss of roof structural detail
- Omission of 15% of buildings (small & large)
- Loss of form & generalisation
- Can detect new buildings (even small)

***Factors:** shadows, resolution, edge definition, occlusions, noise & artifacts*

3D Model of University of Melbourne Campus from *Ikonos* 1m B&W Stereo

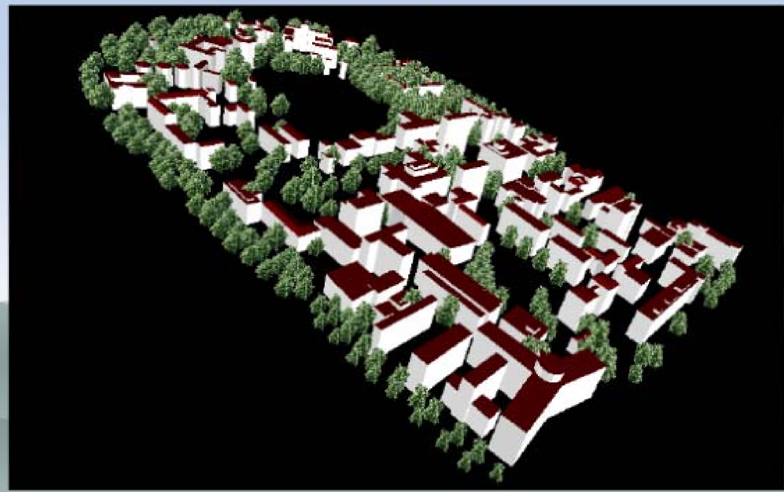

Produced with CyberCity Modeler

Pan-sharpened *Ikonos* 1m ortho-image draped over a DTM

NOAA/AVHRR - MODIS/TERRA Reception, Archiving and Distribution

- NOAA/AVHRR Since 15 November 1997
- TERRA/MODIS Since 25 May 2001
- Archiving all of the received data
- Produce 10days and Monthly NDVI
- Network Data Distribution over Internet for Near Real Time Environment Monitoring

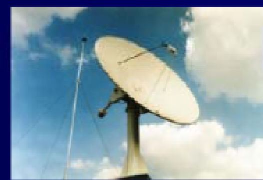

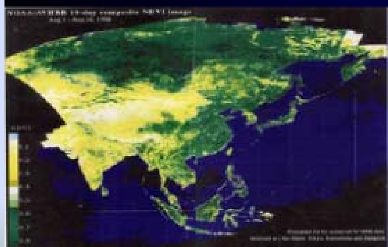

MODIS Installation 22nd May 2001, AIT

MODIS for Flood Monitoring

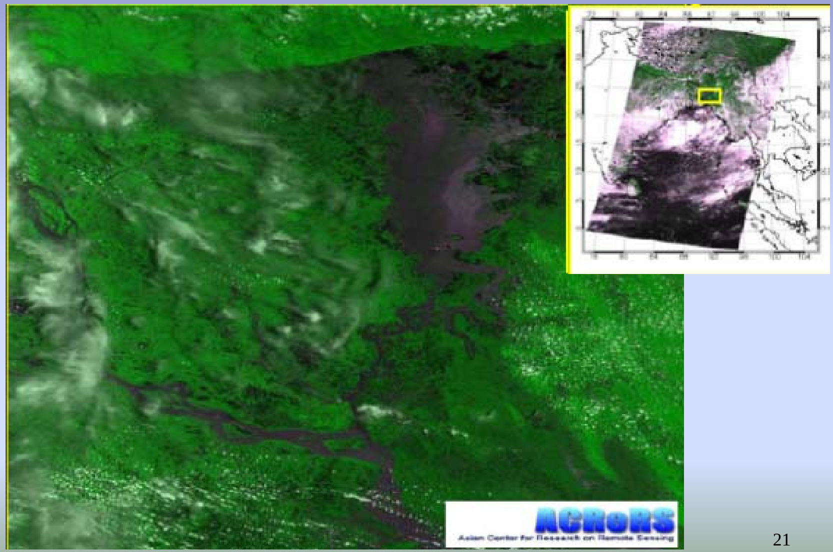

Results - Landuse Classes and its Multi-temporal Spectral Curves

Sample 1 : Perennial Ice

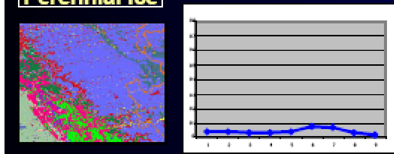

•Northern India

•Vegetation Index is Very low throughout the year

Sample 2 : Bare Land

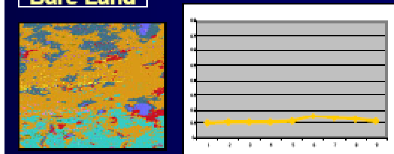

•Tibetan Plateau

•Vegetation index is low throughout the year except for small period of time

Sample 3 : Agriculture Area

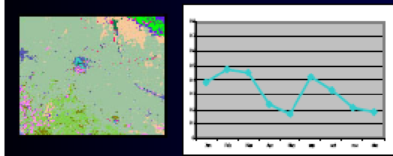

•Central Plain of India

•High Peaks during cropping time

Sample 4 Tropical Forest

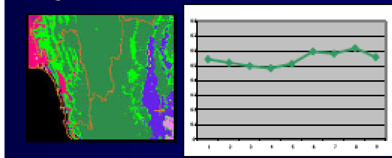

•Forest area in Myanmar

•High vegetation index throughout the year

Planting pattern detection

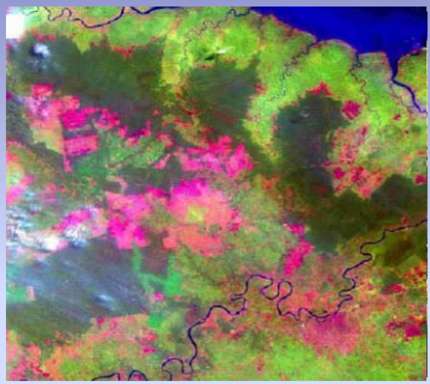

Historical TM image 1989 TM

8 Years Later 1997 TM

Recent TM image for the TREES test site 125/61 on Sumatra
The TM image from 18 August 97 shows new oil palm plantation areas, partly established by replacing old plantations, partly by conversion of forests.

Forest Fire Monitoring from NOAA AVHRR-Thailand

During the period of 4-16 July 2000, many fires were detected in Sumatra and Kalimantan of Indonesia.

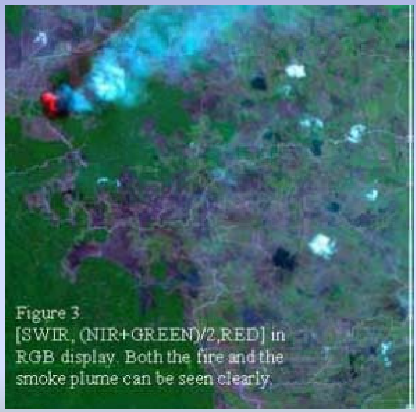

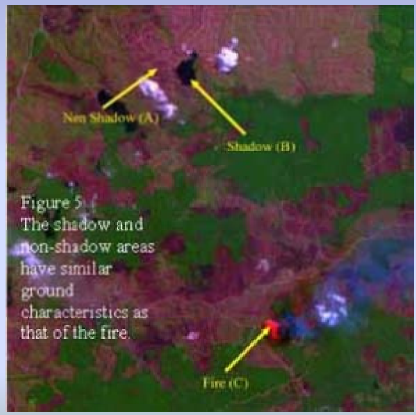

Defense Meteorological Satellite Program[DMSP]

Organizer	Department of Defense(DoD) program run by the Air Force Space and Missile Systems Center(SMC)
Orbit	a sun-synchronous, low altitude polar orbit at the altitude of 830 km / Period 101 min.

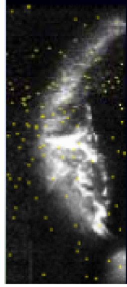

Each DMSP satellite monitors the atmospheric, oceanographic and solar-geophysical environment of the Earth. The visible and infrared sensors collect images of global cloud distribution across a 3,000 km swath during both daytime and nighttime conditions.

Rice Growth Monitoring using RADAR Remote Sensing

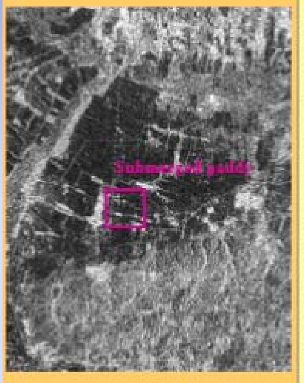

Radar image in March 1997: showing YOUNG PADDY in dark color

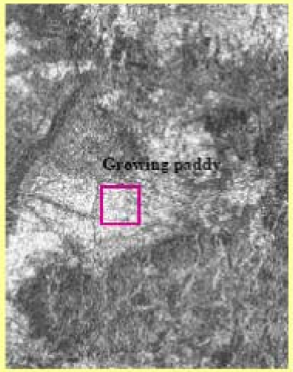

Radar image in May 1997: showing GROWING STATE OF PADDY in bright color

ADEOS image of the same area in May 1997 : TCC showing GROWING STATE OF PADDY

Rice Growth Monitoring Using Near Real Time RADARSAT Fine Beam SAR Data in Pathumthani

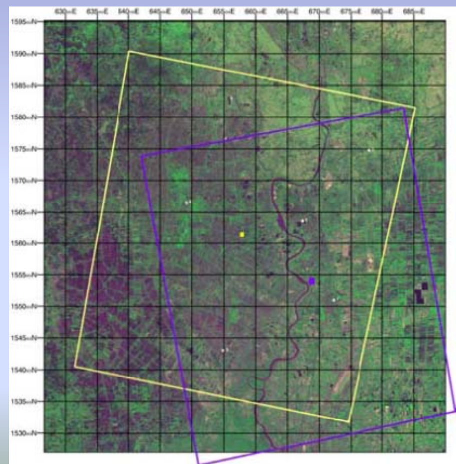

Deployment sites of corner reflectors, plotted On ADEOS AVNIR image

Canada – Japan – Thailand
Within 8 hrs after reception

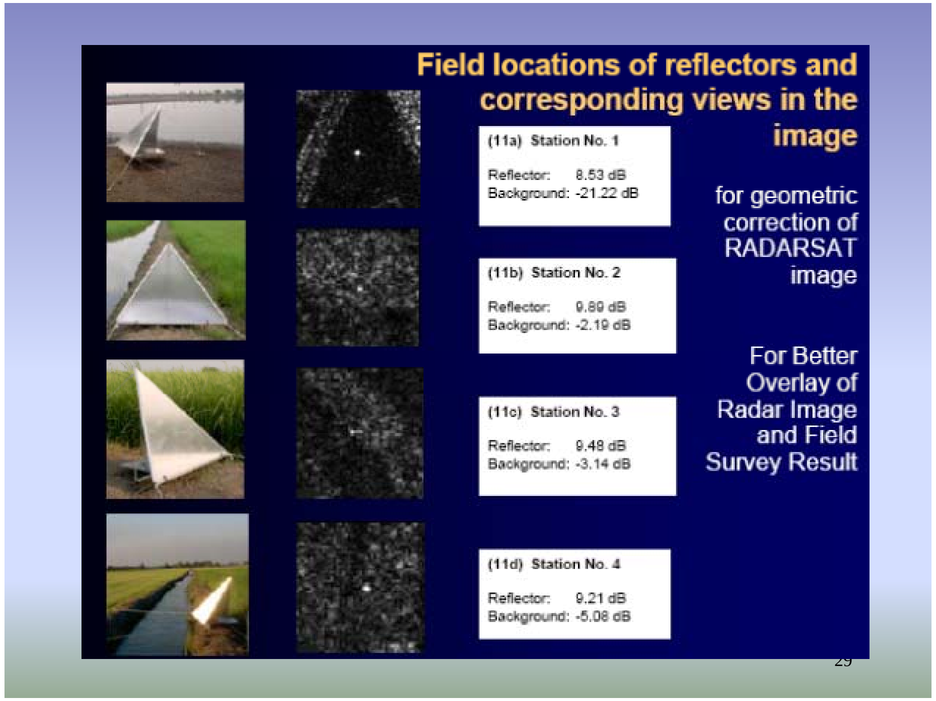
Field locations of reflectors and corresponding views in the image
(11a) Station No. 1
Reflector: 8.53 dB
Background: -21.22 dB
(11b) Station No. 2
Reflector: 9.89 dB
Background: -2.19 dB
(11c) Station No. 3
Reflector: 9.48 dB
Background: -3.14 dB
(11d) Station No. 4
Reflector: 9.21 dB
Background: -5.08 dB
for geometric correction of RADARSAT image
For Better Overlay of Radar Image and Field Survey Result
29

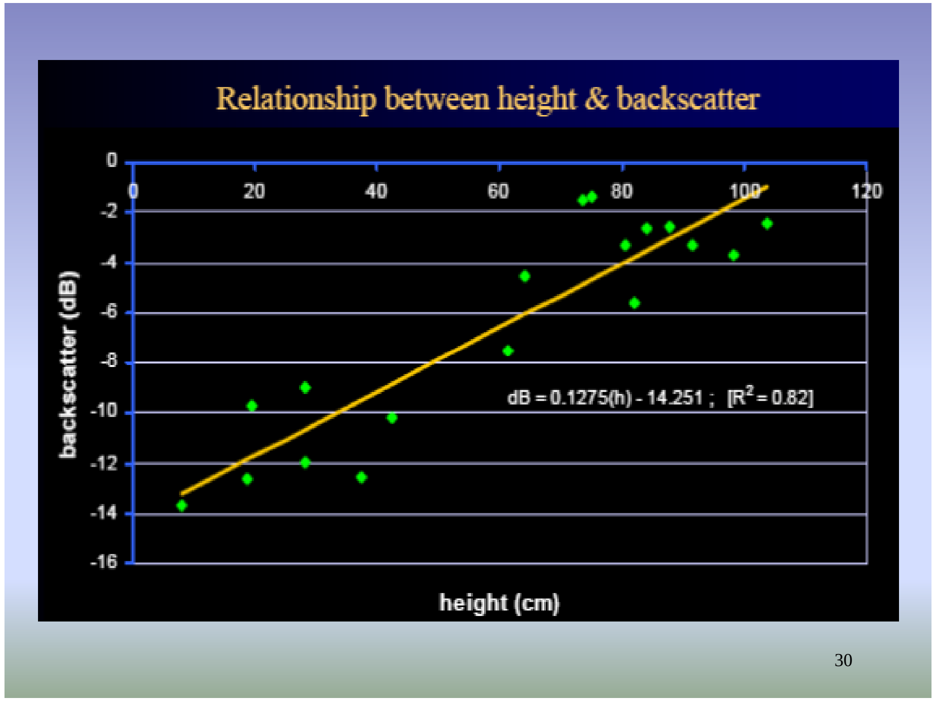
Relationship between height & backscatter
backscatter (dB)
height (cm)
dB = 0.1275(h) - 14.251 ; [R2 = 0.82]
0
-2
-4
-6
-8
-10
-12
-14
-16
0
20
40
60
80
100
120
30

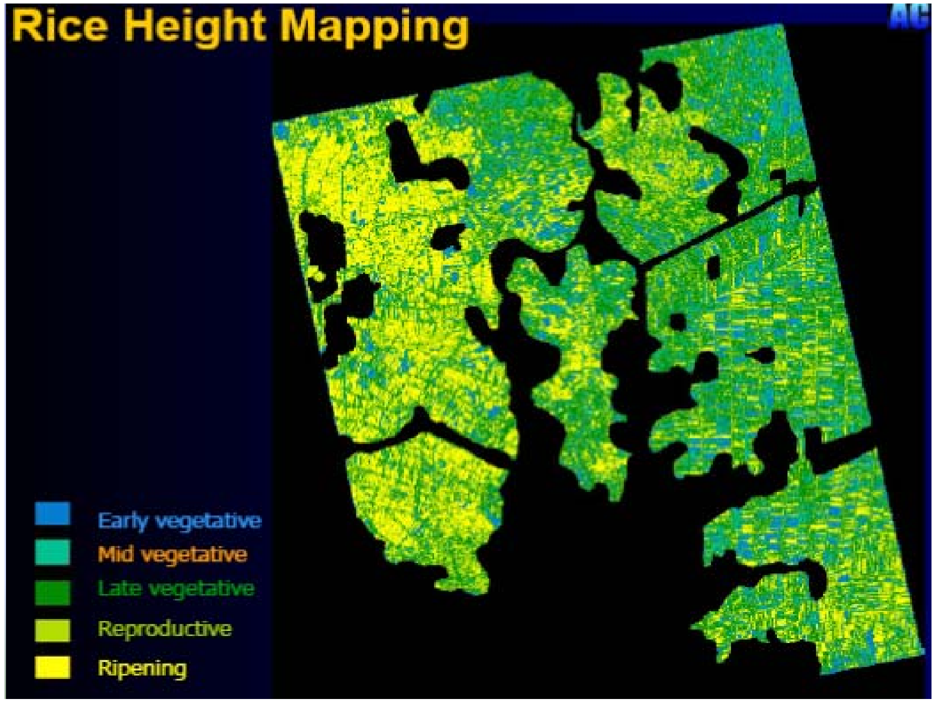
Rice Height Mapping
Early vegetative
Mid vegetative
Late vegetative
Reproductive
Ripening

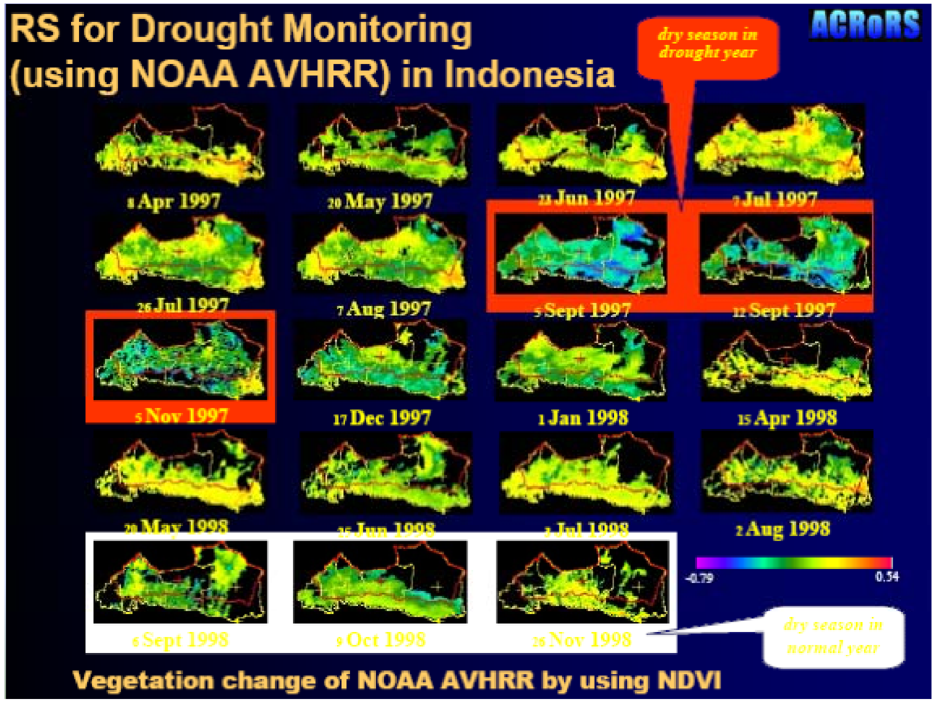
RS for Drought Monitoring (using NOAA AVHRR) in Indonesia
ACRoRS
dry season in drought year
8 Apr 1997
20 May 1997
23 Jun 1997
9 Jul 1997
26 Jul 1997
7 Aug 1997
5 Sept 1997
12 Sept 1997
5 Nov 1997
17 Dec 1997
1 Jan 1998
15 Apr 1998
2 Aug 1998
6 Sept 1998
9 Oct 1998
28 Nov 1998
-0.79
0.54
dry season in normal year
Vegetation change of NOAA AVHRR by using NDVI

Soil-Water-Atmosphere-Plant Model (SWAP)

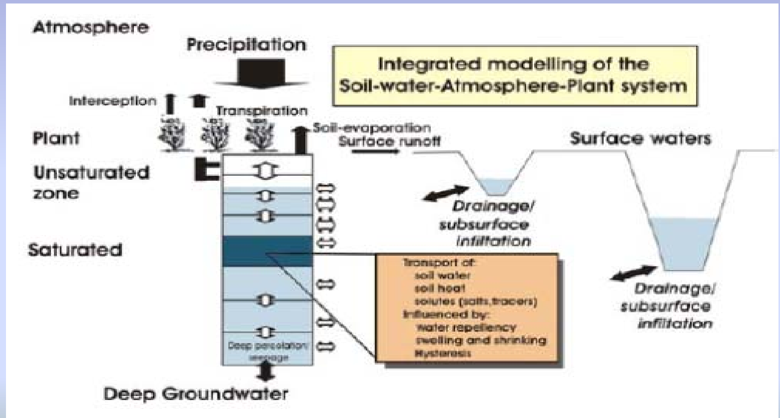

SWAP Model Parameter Determination
- Data Assimilation using RS and GA -

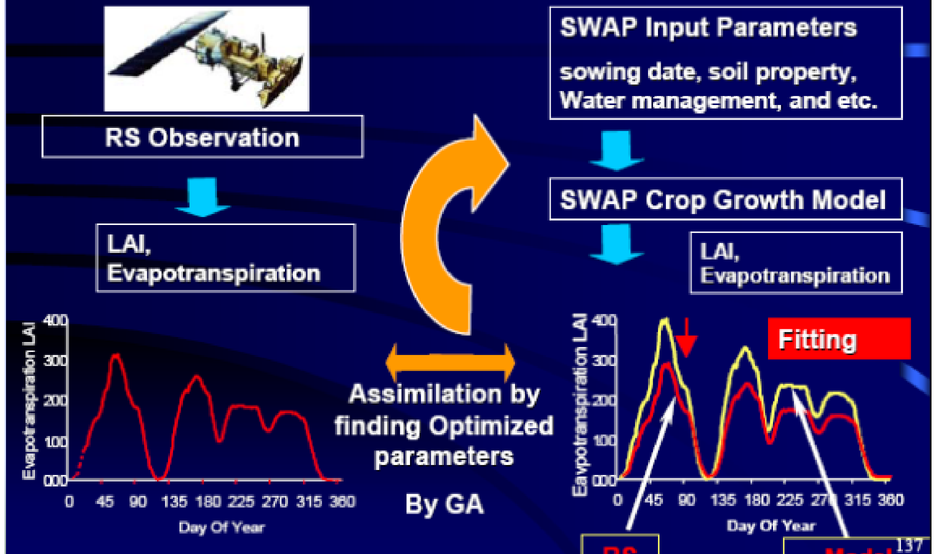

Soil moisture measurement

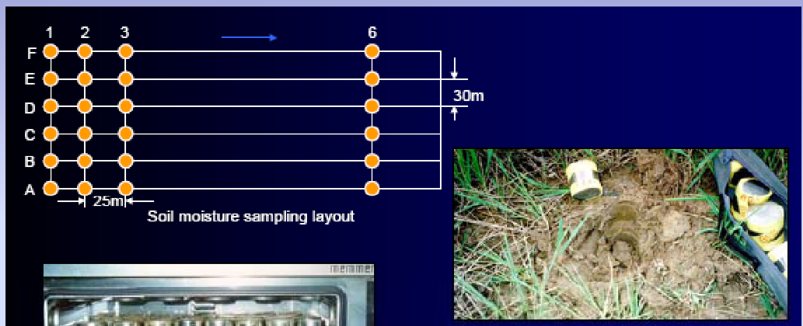

Soil moisture sampling layout

Soil sample collected at a sampling point using a 100-cc core barrel

Soil samples oven-dried for 24 hours at 105 °C

Remote Sensing for Coastal Zone Management
Shrimp Farm extension in Chantaburi(1987- 1995)

February 1987:LandSat-TM August 1997: ADEOS-AVNIR

Remote Sensing for Coastal Zone Management Shrimp Farm extension in Chantaburi(1987- 1995) Extent of shrimp cultivation increase within ten years period in Chantaburi coastal area is clearly visible. Area shown within yellow square/circle in 1997 image are the area converted to shrimp farms.

Soil Erosion Monitoring

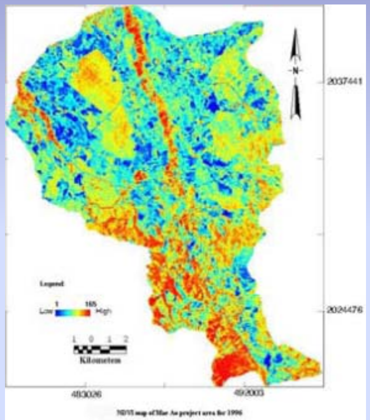

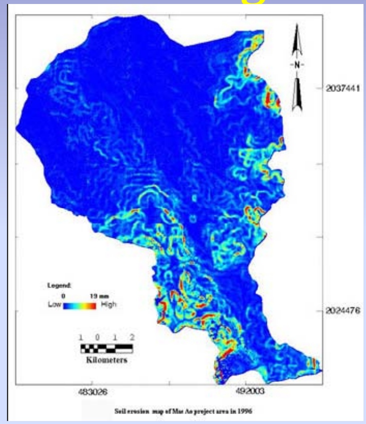

NDVI Map (Normalized Differential Vegetation Index)

Soil Erosion rate 0.91 mm/year

Soil Erosion Map

Model for estimating yield using LAI, topographic and meteorological variables

Considered parameters :
Yield, satellite image derived LAI, topographic and meteorological variables

Method :
- assigning weights for each parameter
- the relationship between average yield and weight of each parameter

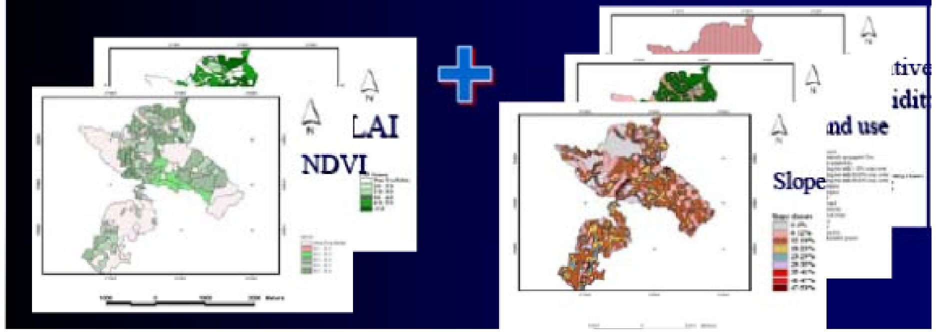

Develop a model to find the correlation between LAI and NDVI derived from spectrophotometer readings

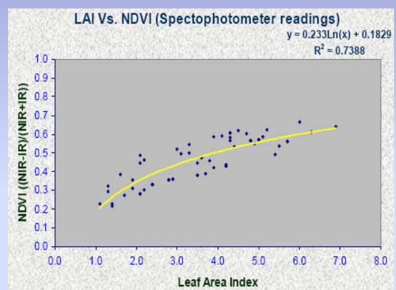

Tea yield Model

$$Yield = -603.923 + 50.124w_d - 23.5w_r - 14.049w_l + 65.845w_i + 513.54w_a + 39.54w_h + 65.695w_f + 46.338w_e$$

Where;
w_d = Soil depth weight; w_r = Rockiness cover weight; w_l = Landuse type weight
w_i = LAI weight; w_a = Age of tea plantation weight; w_h = Relative humidity weight
w_f = Rainfall weight; w_e = Elevation weight

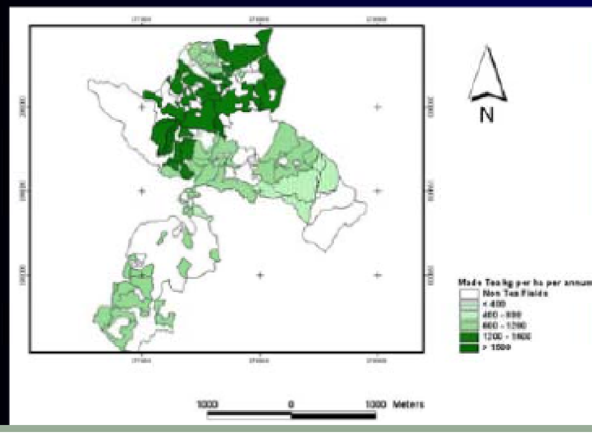

Accuracy = 95%

Predicted average yield map for year 2000 for Westhall estate: 2000 - 1084 kg made tea ha^{-1}

Mt. Mayon Volcano Comprehensive Disaster Prevention Master Plan

GIS Data Development for Planner
- Historical River planform Change by lava, pyroclastic flow, lahar
- Sediment Production Estimation for river structure planning

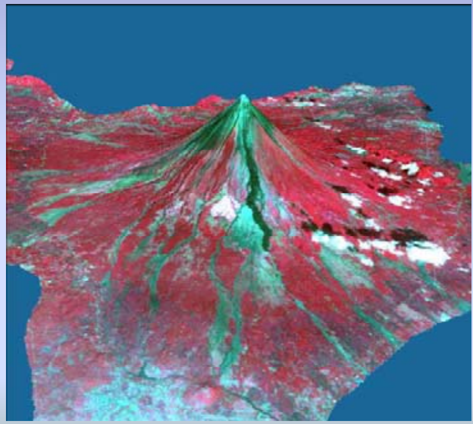

Lava Deposit of Mr. Mayon (Pawa Burabod riverbed)

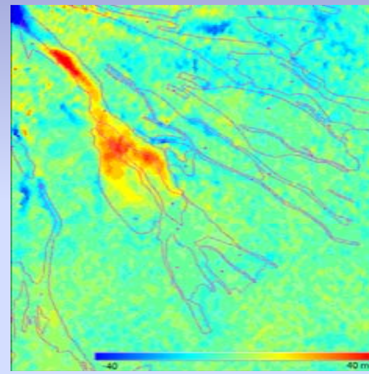

Estimation of Lava Deposit Height using SAR Interferometry
INSAR result Topographic difference

Flood Monitoring using JERS SAR 12 Scenes Mosaic

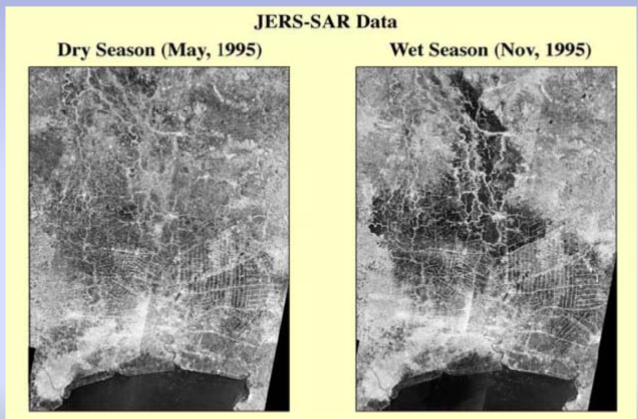

Bangkok Urban Area Expansion 1988 - 1999

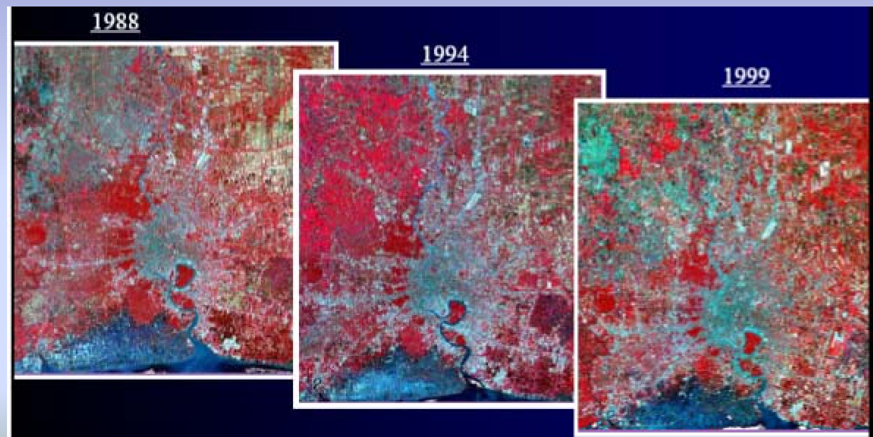

Urban extent from 1988 to 1999 using classified Landsat TM

Military

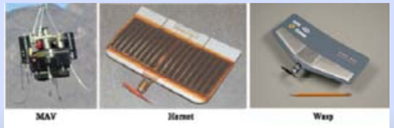

Micro Air Vehicles (MAV)

GPS

Global Navigation Satellite Systems (GNSS)

- NAVSTAR
  - USA
- GLONASS
  - Russians
- Galileo
  - Europeans

How GPS works?

- Range from each satellite calculated
  range = time delay X speed of light
- Technique called trilateration is used to determine you position or “fix”
  - Intersection of spheres
- At least 3 satellites required for 2D fix
- However, 4 satellites should always be used
  - The 4th satellite used to compensate for inaccurate clock in GPS receivers
  - Yields much better accuracy and provides 3D fix

Three SV ranges known

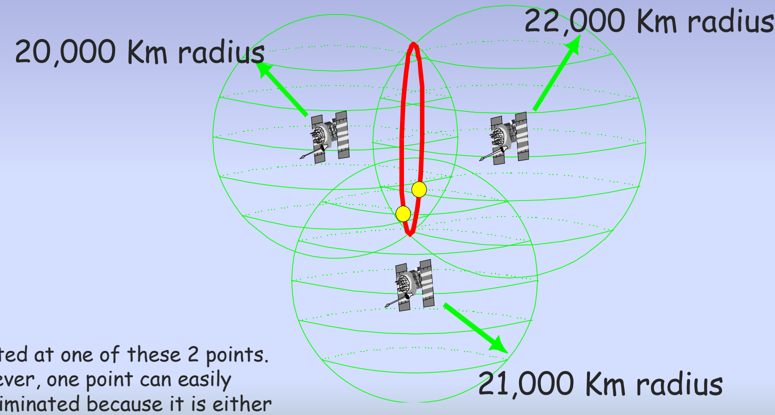

Located at one of these 2 points. However, one point can easily be eliminated because it is either not on earth or moving at impossible rate of speed.

Debris flow

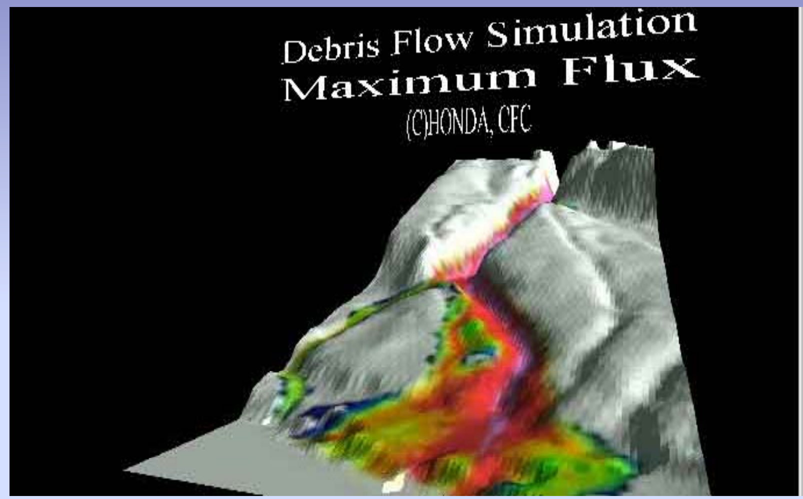

http://www.star.ait.ac.th/~honda/debris.html

21 Urban heat Island

- While the problems of stratospheric ozone depletion and climate change are global in scale, acid deposition, another air-related environmental problem, is regional.
- **Regional - Acid Rain**
- The composition of rain and snow depends upon the gases or other agents present in region of the atmosphere in which the clouds are formed. When water forms clouds, various chemicals and dust particles (both naturally-occurring and anthropogenic) are dissolved or trapped in the droplets, and eventually deposited back onto the ground.
- "Natural" acidity occurs because of dissolved organic oxides (like CO2) and sulfur compounds from decaying biomass. Acidity also occurs as a result of more extreme phenomena like volcanic eruptions, which spew large quantities of CO2, H2S, and SO2 into the air

Local - Photochemical Smog & Tropospheric Ozone

- Smog (SMoke and fOG) was a phenomenon recognized in the early 1950's when thousands of deaths and intense respiratory problems occurred in London, England; Donora, Pennsylvania; and cities in other countries all over the industrialized world.

- Among the gases produced in the photochemical smog are ozone and peroxyacetyl nitrate (often referred to as PAN). The following reactions produce ground-level ozone:
- NO_2 + uv NO + O
  O + O_2 (+ catalyst) O_3 (+ catalyst)

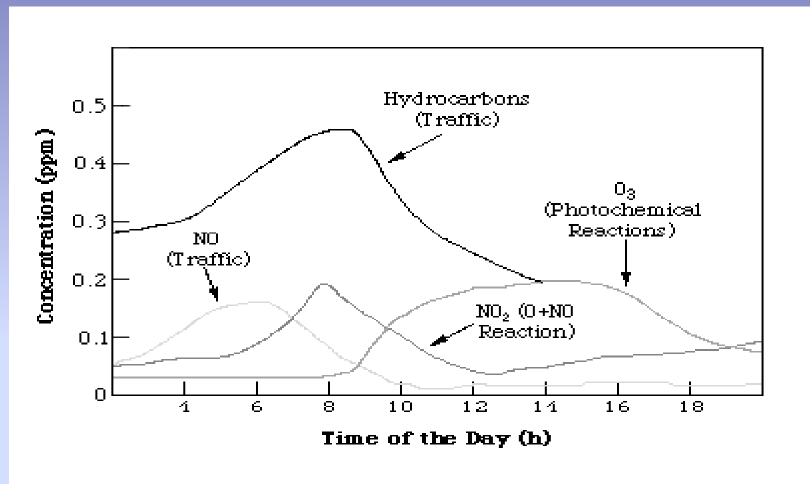

Rise of ozone smog toward mid day.

Local - Urban Heat Islands

- Urban heat islands" are a sort of localized enhanced greenhouse phenomenon. They are simply built-up areas of city that are significantly warmer than the surrounding area of countryside. The difference in temperature comes from the fact that buildings, paved surfaces, and other man-made structures absorb higher amounts of sunlight than most natural objects. This energy is re-radiated at longer wavelengths during the night, and atmospheric pollution in the form of heat-absorbing gases form a "local" atmosphere much like the glass of a greenhouse, trapping in the heat.

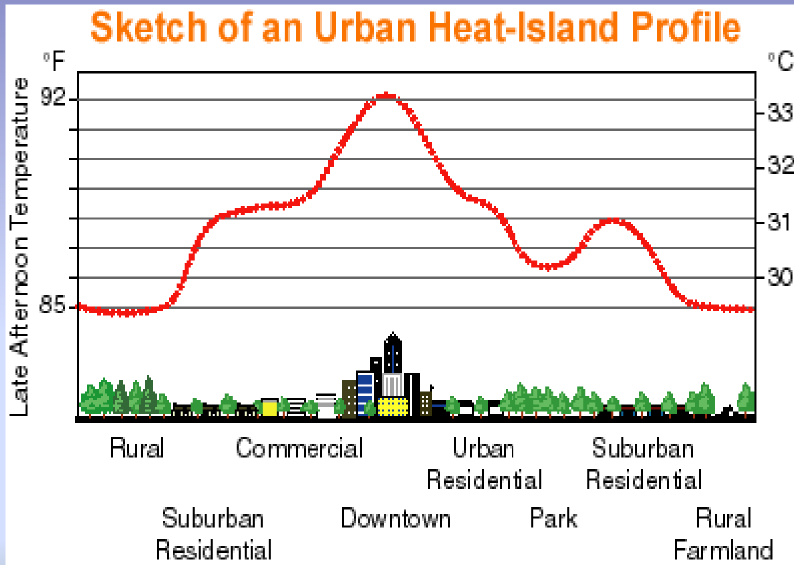

Remote Sensing of the Urban Heat Island Effect across Biomes in the Continental USA

In Environmental Science, Imagery, Spatial Analysis on April 21, 2010 at 6:29 am

Remote Sensing of Environment, Volume 114, Issue 3, 15 March 2010, Pages 504-513

Imhoff, M.L., Zhang, P., Wolfe, R.E. and Bounoua, L

"Impervious surface area (ISA) from the Landsat TM-based NLCD 2001 dataset and land surface temperature (LST) from MODIS averaged over three annual cycles (2003–2005) are used in a spatial analysis to assess the urban heat island (UHI) skin temperature amplitude and its relationship to development intensity, size, and ecological setting for 38 of the most populous cities in the continental United States. Development intensity zones based on %ISA are defined for each urban area emanating outward from the urban core to the non-urban rural areas nearby and used to stratify sampling for land surface temperatures and NDVI. Sampling is further constrained by biome and elevation to insure objective intercomparisons between zones and between cities in different biomes permitting the definition of hierarchically ordered zones that are consistent across urban areas in different ecological setting and across scales.

- http://gisandscience.com/2010/04/21/remote-sensing-of-the-urban-heat-island-effect-across-biomes-in-the-continental-usa/

Reference:

Assoc.Prof.Dr.HONDA Kiyoshi, Lecture Note .School of Engineering and Technology ,AIT Thailand.

Suggested Web Sites:

- AUSLIG (http://www.auslig.gov.au/)
- Space Imaging (http://www.spaceimage.com/)
- Australian Bureau of Meteorology (http://www.bom.gov.au/sat/intro/paper1intro.shtml)
- JPL Radar Site (http://www.jpl.nasa.gov/radar/sircxsar/)
- Australian geological Survey Organization (http://www.agso.gov.au/)

Question?

Thank you for your kind attention